Intern. J. Environ. Anal. Chem., 2014
Vol. 94, No. 4, 332–347, http://dx.doi.org/10.1080/03067319.2013.840886

Taylor & Francis
Taylor & Francis Group

A more accurate analysis of alkylated PAH and PASH and its implications in environmental forensics

Patrick M. Antle, Christian D. Zeigler, Nicholas M. Wilton and Albert Robbat, Jr.*

Tufts University, Department of Chemistry, Medford, MA, USA

(*Received 11 March 2013; final version accepted 17 August 2013*)

The accurate measurement of polycyclic aromatic hydrocarbons (PAH), polycyclic aromatic sulfur heterocycles (PASH), and their alkylated homologues is essential at all levels of risk assessment and remedial decision-making. In the field of environmental forensics, diagnostic ratios of these compounds are used to delineate fossil fuel-based sources from one another and to assess the degree of weathering occurring on-site. Fresh and weathered coal tar and crude oil samples from different locations were analysed by gas chromatography/mass spectrometry. The same files were analysed by selected ion extraction of one-ion and two-ion signals from full-scan data and compared to a new data analysis method using spectral information from homologous isomers. Findings showed that using too few ions produced false positives and concentrations much higher than those found using the homologous isomer spectral method, which adversely affected the corresponding diagnostic ratios used by forensic scientists.

Keywords: alkylated PAH; alkylated PASH; PAH_{34}; diagnostic ratios; environmental forensics; fragmentation patterns; oil spill fingerprinting; weathering; GC/MS

1. Introduction

Polycyclic aromatic hydrocarbons (PAH) and their alkylated homologues are pervasive environmental pollutants. They exist as a result of fossil fuel combustion, natural oil seeps, asphalt and shingle runoff, petroleum recovery, storage and transport activities, and from past actions at manufactured gas plants (MGP). PAH are among the most-studied pollutants, with their source, transport, plant and animal uptake, toxicity, and fate in the environment all of the utmost importance. For example, the U.S. Environmental Protection Agency (EPA) measures the concentration of 16 'parent' PAH and 18 alkylated naphthalene, fluorene, phenanthrene, pyrene, and chrysene homologues, known as the $\Sigma PAH_{34,}$ to estimate the toxic hazard of contaminated soils and sediments [1,2]. In addition to PAH [3,4], polycyclic aromatic sulfur heterocycles (PASH) such as dibenzothiophene (DBT) and its C_1 to C_4 alkylated homologues also serve as indicators of persistence and damage to the environment [5].

Fossil fuel pollutants weather differently in the environment; how they weather determines their immediate and eventual impact on local ecosystems [6]. At some sites, source material pollutants have seeped into sediment for decades, with weathering processes partitioning some components and transforming others. These processes include evaporation, dissolution, emulsification, adsorption, and microbial degradation, among others [7]. Volatility, solubility, adsorption, and resistance to environmental degradation vary dramatically from homologue to homologue, even from isomer to isomer within the same homologue [8]. This variability

*Corresponding author. Email: Albert.Robbat@Tufts.edu

makes it difficult to predict how PAH and PASH concentrations change in the environment; understanding these processes is critical to site remediation strategies.

Chemical fingerprints of source materials (unweathered samples) and impacted (weathered) samples play a major role in environmental forensics. For more than 30 years, investigators have used diagnostic ratios, based on individual and homologue-specific PAH and PASH concentrations, to support site investigation and cleanup projects and litigation [9]. For example, forensic scientists use diagnostic ratios to identify and differentiate one source material from another and to estimate the amount of weathering that has occurred [10]. These assessments rely on the principle that each source has a unique chemical composition with a recognisable PAH/PASH distribution pattern, and that changes in concentration over time, owing to physical, chemical, and biological processes, can affect ecosystem toxicity and, thus, cleanup strategy [11]. PAH/PASH ratios that are constant over time are useful in delineating source identity, and those that change substantially provide an estimate of how much the source material has weathered. In 1999, Wang and coworkers published an authoritative review in which they state that alkylated PAH homologues are the 'backbone of chemical characterisation and identification of oil spill assessments' [10]. Forensic scientists and toxicologists rely on accurate methods of PAH and PASH analysis, as errors in peak assignments produce inaccurate concentration estimates, which, in turn, lead to incorrect diagnostics and costly site remediation activities.

Gas chromatography/mass spectrometry (GC/MS) is the technique most often used to quantify PAH and PASH [10,12,13]. To increase measurement sensitivity of low concentration analytes, such as the C_3 and C_4 homologues, analysts typically operate the MS in selected ion monitoring (SIM) mode [14]. SIM analysis is an acceptable alternative to full-scan mass spectrometry when full-scan MS is incapable of detecting target compounds below the limits of quantitation needed to answer site-specific questions. Because SIM methods typically monitor one or two ions per homologue, they can provide a lower degree of confidence owing to the loss of spectral information [15]. Thus, analysts rely on pattern recognition of alkylated PAH and PASH ion chromatograms within specified retention windows, which can result in overestimated concentrations owing to additive ion effects from the matrix. For example, we showed that if *m/z* 208 is the only ion used to identify C_3-fluorene isomers, homologue concentrations will be overestimated because electron impact fragmentation of the C_2 and C_3 three-ring alkylated PASH, among other homologues in crude oil, coal, and their byproducts, also produce *m/z* 208 and elute in the same retention window as the C_3-fluorene homologue [16].

The scientific community, state and federal agencies, and the private sector rely heavily on SIM data to draw conclusions on the impact of PAH and PASH in the environment. For example, a search of the primary literature reveals nearly 75% of all research published over the last 20 years employed SIM detection and that methods such as those published by ASTM [17] and NOAA [18] prescribe one-ion detection. Recently, we analysed several coal tar and crude oil samples and showed that, owing to incorrect peak assignments, SIM/1-ion analyses overestimate alkylated PAH and PASH concentrations and produce an unacceptable number of false positives compared to full-scan data analysis [19,20]. We also found that if one fragmentation pattern per homologue is used to quantify C_2 to C_4 alkylated PAH, concentrations are underestimated compared to using three-to-five ions per isomer pattern and multiple fragmentation patterns per homologue (MFPPH) [21].

To determine the minimum number of spectral patterns needed to correctly identify all isomers within each PAH and PASH homologue and to obtain their corresponding retention windows, crude oil and coal tar samples from different geographic locations were analysed by automated sequential GC-GC/MS. Once the retention windows and mass spectral libraries from

actual samples were obtained, we confirmed findings by analysing 119 two-to-five-ring PASH compounds [16] synthesised by Andersson [22] and Lee [23]. As a result, we developed a full-scan method that employs multiple fragmentation patterns per homologue to quantify alkylated PAH and PASH [19,20].

Environmental forensic studies rely on a multi-tiered analytical approach that includes GC/FID and stable isotope ratio analyses in addition to compound-specific GC/MS analysis of PAH, PASH and biomarkers. The objective of this study is to examine the effects of PAH and PASH concentration differences produced by one- and two-ion detection or selected ion extraction (SIE) methods versus analysis by MFPPH ions on the diagnostic ratios used in environmental forensics. Results show that the use of too-few ions leads to inaccurate concentration estimates, incorrect diagnostic ratios, and falsely considered assessments, and that meaningful forensic studies should employ MFPPH analysis independent of MS detection mode. This paper is the first comprehensive SIM/SIE vs. MFPPH assessment of the impact on the diagnostic ratios commonly used by forensic chemists.

2. Experimental

2.1 *Standards and reagents*

The 16 EPA-priority pollutant PAH standards, internal standards (1,4-dichlorobenzene-d_4, naphthalene-d_8, phenanthrene-d_{10}, chrysene-d_{12}, and perylene-d_{12}), and activated copper were purchased from Restek (Bellefonte, PA). Anhydrous sodium sulfate, neat dibenzothiophene (DBT), and the base/neutral surrogate mixture (2-fluorobiphenyl, nitrobenzene-d_5, p-terphenyl-d_{14}) were purchased from Sigma-Aldrich (St. Louis, MO). Airgas (Salem, NH) supplied the ultra-high purity helium and nitrogen.

2.2 *Samples*

ONTA (Toronto, Ontario, Canada) supplied the Merey and Orinoco crude oils. Zhendi Wang from Environment Canada (Ottawa, Ontario, Canada) provided the weathered Arabian crude oil sample. We obtained unweathered coal tar from MGP sites in North Carolina and Illinois. Coal tar contaminated soils were obtained from the same site in Illinois and from a site in Wisconsin, and contaminated sediment from the Hudson River in New York. Environmental engineering companies collected these samples and shipped them overnight on ice to the university, where they were stored at 3°C until analysed.

2.3 *Sample preparation full-scan*

We followed the prescribed extraction procedure for soil and sediment samples as described in EPA methods 3550C and 3660B. Briefly, borosilicate glass vials (Fisher Scientific, Pittsburgh, PA) containing 15 g of soil or sediment spiked with base/neutral surrogate spike mix and 8 mL of 50% toluene/50% dichloromethane (v/v) were sonicated for 10 min (Branson 2210, Danbury, CT). After removing the extract and adding fresh solvent each time, the sonication procedure was repeated 7-times to ensure maximum extraction efficiency. For soils, the filtered extract was concentrated under a steam of nitrogen. For sediments, addition of activated copper and anhydrous sodium sulfate to the filtered extract removed elemental sulfur and water before concentration under a stream of nitrogen. A known quantity of the internal standard mixture was added to the extract before it was analysed.

2.4 *Instrumentation*

An Agilent Technologies (Santa Clara, CA) 6890/5973 GC/MS with a Gerstel (Mülheim an der Ruhr, Germany) MPS2 autosampler and CIS6 PTV inlet and a Shimadzu (Columbia, MD) GC2010/QP2010+ GC/MS, each with an RTX-5MS 30 m × 0.25 mm ID × 0.25 μm column from Restek, were used in this study. Instrument operating conditions were as follows: for the Shimadzu GC, 1 μL splitless sample injection, 1 mL/min constant helium flow, 60°C (1 min) to 330°C at 5°C/min temperature programme, with MS conditions of 50–350 *m/z* scan range at 8.3 Hz; and for the Agilent GC, 1 μL splitless injection, 268 kPa constant pressure helium flow, 60°C (1 min) to 330°C at 5°C/min temperature programme, and MS of 50–400 *m/z* scan range at 5 Hz.

2.5 *Data analysis*

Known concentrations of the 16 EPA-priority PAH and DBT standards were serially diluted and analysed to obtain the method detection limit and average response factor (RF) over the concentration range. The linear calibration range was based on a minimum of eight points over the concentration range of 0.2–25 μg/mL for the 2- and 3-ring PAH and 0.4–25 μg/mL for the larger PAH. Calculation of the RF at each concentration was $A_X C_{IS}/A_{IS} C_X$, where C_X is the concentration of PAH injected, A_X the observed signal for said injection, and C_{IS} and A_{IS} are the corresponding internal standard concentration and signal response. The same average RF was used for both SIM and MFPPH analyses. We found the average RF over the calibration range for parent PAH was less than 15%, with these values used to calculate concentrations of the corresponding alkylated homologues.

All samples were analysed by full-scan mass spectrometry, followed by extraction of 1-, 2- and MFPPH ion signals from the same data file. For SIM/1-ion, the molecular ion, and for SIM/2-ion, the molecular and most abundant confirming ions were used for C_1 to C_4 alkylated naphthalene, fluorene, phenanthrene, pyrene, chrysene, and dibenzothiophene. Those peaks that contained these ions found within the retention windows were integrated. For MFPPH, we used the recently published PAH and PASH spectral patterns and retention windows [16,19,20]. In this study, new spectral deconvolution data analysis software developed by Ion Analytics (Andover, MA) was used to analyse the data. The deconvolution algorithms that form the foundation of this software have been described previously [24]. The software's compound identification criterion is a three-fold confirmation process. First, detection of each homologue's spectral patterns, i.e., ions and relative abundances, must comaximise and be ≤ 20% at each scan across the peak. This criterion ensures that the spectra are invariant across the peak. Second, the Q-value must be ≥ 90. The Q-value is a measure of the deviation between the expected and observed ion ratios for each ion across the peak and ranges between 1 and 100. The higher the Q-value, the higher the certainty that sample and library spectra match one another. Finally, the Q-ratio, the peak area ratio of the base and confirmation ions, must be ≤ 20% of the library relative abundance for each spectral pattern to confirm compound identity. Only the molecular ion signal from those scans that meet all three criteria are extracted from the peak are used to quantify the homologues.

3. Results and discussion

Figure 1 shows the overlap in PAH and PASH retention windows from which analysts must recognise homologue-specific peak patterns. Also shown are those homologues whose fragmentation ions interfere with the quantification ion of a specific homologue if a single ion is

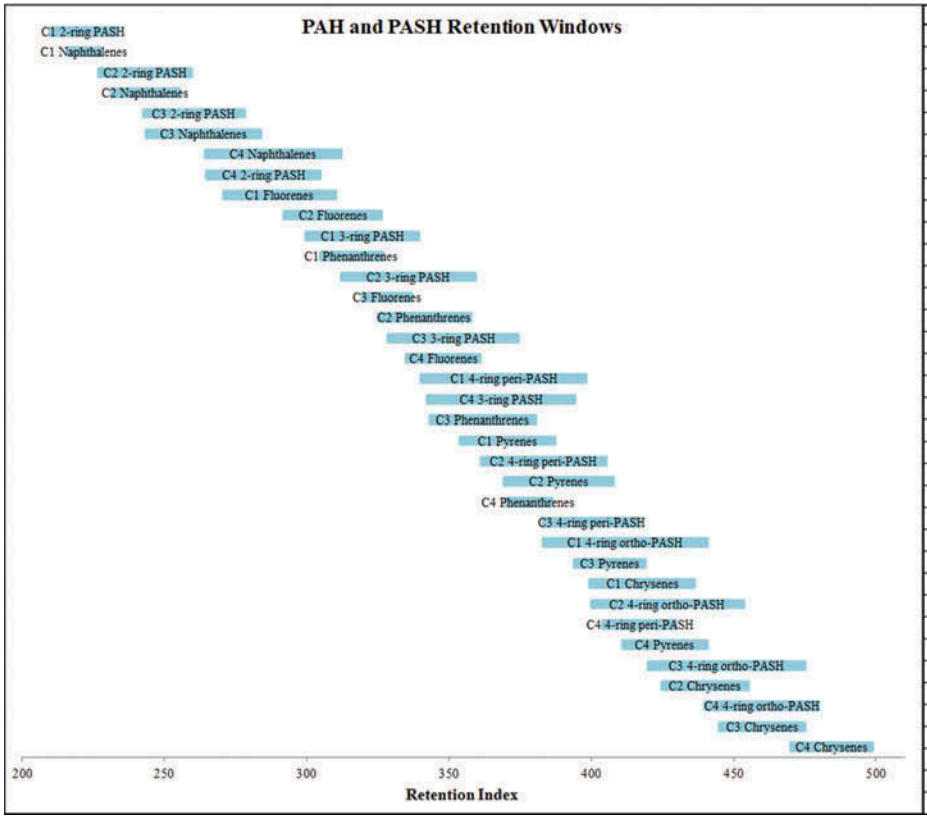

Homologue	Quant Ion	Interfering Homologues
C_1 2-ring PASH	148	C_2 2-ring PASH
C_1 Naphthalenes	142	C_2 Napthalenenes
C_2 2-ring PASH	162	C_3 2-ring PASH, C_4 2-ring PASH
C_2 Naphthalenes	156	C_3 Naphthalenes
C_3 2-ring PASH	176	C_4 2-ring PASH
C_3 Naphthalenes	170	C_4 Naphthalenes
C_4 Naphthalenes	184	C_0 3-ring PASH, C_2 3-ring PASH
C_4 2-ring PASH	190	C_1 Phenanthrenes
C_1 Fluorenes	180	C_2 Fluorenes
C_2 Fluorenes	194	C_3 Fluorenes, C_4 Fluorenes
C_1 3-ring PASH	198	C_2 3-ring PASH
C_1 Phenanthrenes	192	C_2 Phenanthrenes
C_2 3-ring PASH	212	C_3 3-ring PASH, C_0 4-ring *ortho*-PASH
C_3 Fluorenes	208	C_4 Fluorenes, C_2 3-ring PASH, C_3 3-ring PASH
C_2 Phenanthrenes	206	C_3 Phenanthrenes
C_3 3-ring PASH	226	C_4 3-ring PASH, C_0 Chrysene
C_4 Fluorenes	222	C_1 4-ring *peri*-PASH
C_1 4-ring *peri*-PASH	222	C_4 Fluorenes
C_4 3-ring PASH	240	C_1 Chrysenes, C_0 4-ring *ortho*-PASH
C_3 Phenanthrenes	220	C_4 Phenanthrenes, C_1 4-ring *ortho*-PASH
C_1 Pyrenes	216	C_2 Pyrenes
C_2 4-ring *peri*-PASH	236	
C_2 Pyrenes	230	C_3 Pyrenes
C_4 Phenanthrenes	234	C_2 4-ring *peri*-PASH, C_0 4-ring *ortho*-PASH
C_3 4-ring *peri*-PASH	250	C_0 5-ring PAH
C_1 4-ring *ortho*-PASH	248	C_3 4-ring *peri*-PASH
C_3 Pyrenes	244	C_4 Pyrenes, C_0 4-ring *ortho*-PASH
C_1 Chrysenes	242	
C_2 4-ring *ortho*-PASH	262	
C_4 4-ring *peri*-PASH	264	
C_4 Pyrenes	258	
C_3 4-ring *ortho*-PASH	276	C_0 6-ring PAH
C_2 Chrysenes	256	C_4 4-ring *peri*-PASH, C_0 5-ring PAH
C_4 4-ring *ortho*-PASH	290	
C_3 Chrysenes	270	
C_4 Chrysenes	284	C_0 5-ring PASH

Figure 1. Retention windows and quantitation ion interferences for alkylated PAH and PASH; bar behind homologue name indicates retention window.

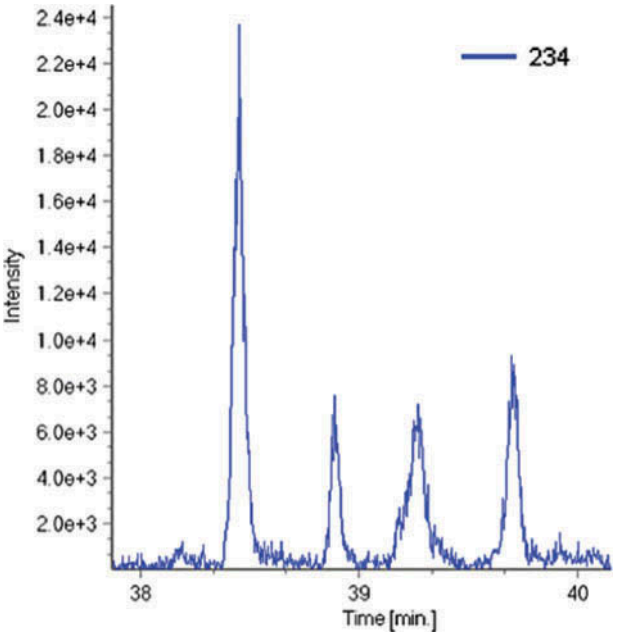

Figure 2. *m/z* 234 ion trace from a coal tar contaminated soil, SOIL.

used to detect the homologue (SIM/1-ion) or is extracted from full-scan data (SIE/1-ion). For purposes of constructing the figure, only fragment ions whose relative abundance is greater than 15% of the homologue's molecular ion are considered. Note that both PAH and PASH interfere with one another. Signal from non-target matrix compounds can also add to the total homologue peak area when reliance on pattern recognition is employed.

Figures 2 and 3 illustrate an example of wrongly assigned peak patterns caused by the detection of too few ions to unambiguously identify target compounds and its effect on homologue concentrations. Figure 2 shows the ion current chromatogram at *m/z* 234, which is the molecular ion for C_4-phenanthrene. A total of four compounds elute within the retention window for this homologue. Detection by SIM or extraction of this ion from full scan GC/MS data would result in these peaks being identified as C_4-phenanthrenes. Examination of this homologue's fragmentation ions, however, reveals that these peaks are the result of matrix interferences. Figure 3 shows the fragmentation ion traces (*m/z* 235, 234, 219, 204, 203, and 189) for the 2,4,5,7- and 3,4,5,6-tetramethylphenanthrenes and the 2,7,9,10-tetramethylphenanthrene isomers, see figure caption for fragmentation pattern relative abundances. Although the reconstructed ion current chromatograms maximise at the peak apexes for some ions, not all fragmentation ions are present; i.e. *m/z* 219, whose relative abundance is 60% and should be evident in the chromatograms. Moreover, the signals of the confirming ions based on their relative abundances should have been well-above instrument noise and do not match those relative abundances listed in the figure caption for these isomers. For example, the *m/z* 235 ion should have relative abundances similar to that of *m/z* 203 in pattern A and *m/z* 204 in pattern B, but does not. As a result, the peaks in Figure 2 are rejected as C_4-phenanthrene compounds when the identification criterion described in the experimental section is employed. In this example, relying solely on the molecular ion to measure C_4-phenanthrene produces a concentration of 220 μg/g. In contrast, MFPPH yields no measurable concentration. According to the EPA equilibrium partitioning sediment benchmark model, 220 μg/mL of C_4-phenanthrene corresponds to 0.34 toxic units for a sample that contains 1% total organic carbon

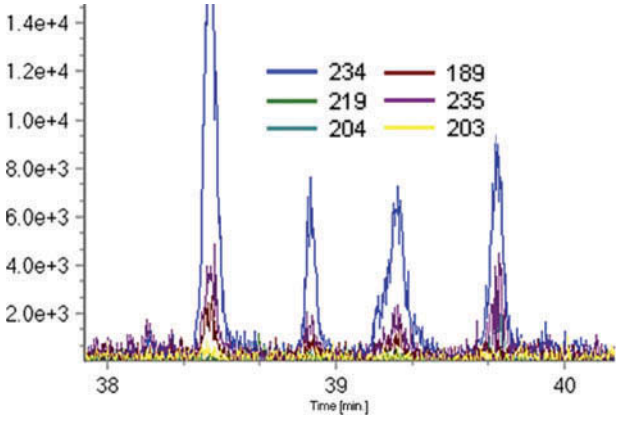

Figure 3. C_4-phenanthrene fragmentation ions and their relative abundances; *m/z* 234 (100%); 219 (75); 204 (31%); 203 (23%); 235 (20%) for the 2,4,5,7- and 3,4,5,6-tetramethyl isomers (pattern A) and *m/z* 234 (100%); 219 (60%); 235 (21%); 204 (17%); 189 (13%) for the 2,7,9,10-tetramethyl isomer (pattern B). Also shown are the reconstructed ion chromatograms from the sample in Figure 2.

[2]. As a toxic unit of 1 is the threshold for ascribing potential soil/sediment toxicity, the C_4-phenanthrene homologue concentration would have added one-third of the toxic equivalent to a site contaminated with crude oil or coal tar when, in fact, the homologue should not have contributed to site toxicity at all. This finding is problematic, because more than 50% of the publications we reviewed relied on one-ion SIM detection, and is consistent with concerns expressed by others [25,26].

Although inclusion of *m/z* 219 (the most abundant confirming ion) would proscribe inclusion of these peak signals in the C_4-phenanthrene concentration estimate, the addition of a single qualifying ion will not always produce the correct concentration for all homologues. For example, when examining C_2-fluorene in the same sample, both SIM/1-ion at *m/z* 179 and SIM/2-ion at *m/z* 179 and 194 identify several peaks revealed to be false positives by MFPPH when other confirmation ions are included. Moreover, if the confirming ion (as opposed to the molecular ion) is the base ion, as is the case for some isomers of C_3-phenanthrene, concentrations will be underestimated depending on which relative abundance is selected to determine compound identity; see, for example, the trimethyl and methyl-ethyl PAH isomers in reference 20. Some analysts ignore ion ratios and assume that if the two ions comaximise as in the example above, the peak is from a target compound. Still other methods rely on pattern recognition of homologue peaks, which places a significant burden on the analyst to determine which peaks should or should not be included. Such discretion can lead to unpredictable results from one analyst to the next [20].

To examine the effects of this overestimation on environmental forensic diagnostic ratios, we analysed coal tar and crude oil samples and extracted 1-, 2-, and MFPPH ion signals (as a surrogate for SIM analysis) from the same GC/MS data file. Our purpose is to illustrate the differences in the forensic data when too few ions are used; it is not aimed at comparing the differences in measurement sensitivity between full-scan and SIM detection. Such an analysis would introduce an additional error source, whereas using the same data file isolates the differences between the two data analysis methods. Tables 1 and 2 list our findings, which show that the standard SIM analysis biased the diagnostic ratios in every sample. Use of SIM/SIE with too few ions consistently overestimated alkylated homologue concentrations, leading to both positive and negative biases in the diagnostic ratios, which ranged from a few percent to

Table 1. SIM/1-ion vs. MFPPH diagnostic ratio percent bias.

Ratio	Application	Coal tar								Crude oil				
		CTIL	SOIL	CTNC	SDNY1	SDNY2	SOWI1	SOWI2	SOWI3	ME	OR	AR	Min	Max
1.) ΣC/ΣD	Biodegradation [28]	−18	−6	30	−170	−228	−56	−90	−17	FP	34	FP	−228	34
2.) [ΣN + Σ(C0–C3) DBT + (1/2*Σ(C0–C1) P) + Σ(C2–C4)P]/ΣPAH	Biodegradation [29]	1	0	−8	−1	−2	−15	−7	−10	95	−21	−16	−21	95
3.) Pyrogenic Index	Pyrogenic vs. Petrogenic Source [30]	−39	−26	−35	−32	−39	−30	−26	−25	−63	−58	−45	−63	−25
4.) C2D/C2P//C3D/C3P	Source Allocation [31]	−556	−2719	−20	−1969	−2954	−539	−25	−75	15	8	37	−2954	37
5.) ΣP/ΣD	Source Allocation [11]	−53	−27	7	−479	−237	−38	−118	−41	−36	−14	9	−479	9
6.) P/ΣP	Source Allocation [28]	−41	−22	−35	37	−10	−21	−17	−11	−36	−28	−45	−45	37
7.) C1C/C	Source Allocation [28]	40	14	26	5	12	18	4	26	FP	FP	FP	4	40
8.) C2C/C	Source Allocation [28]	54	83	64	76	14	3	FP	6	FP	FP	FP	3	83
9.) C3C/C	Source Allocation [28]	ND	ND	FP	FP	9	FP	FP	FP	ND	ND	ND	9	9
10.) C1D/C1Pyr	Source Allocation [26]	15	0	3	67	1	−8	−8	−3	46	16	23	−8	67
11.) Σ(C2–C4)N/ΣPAH	Source Allocation and Weathering [32]	14	32	7	6	44	40	1	6	95	−15	−21	−21	95
12.) C1P/ΣP	Source Allocation and Weathering [33]	−30	−16	−31	−93	−10	−7	−8	−6	−14	−16	−40	−93	−6
13.) C1D/ΣD	Source Allocation and Weathering [31]	−69	−46	−19	−265	−267	−59	−155	−55	16	−12	1	−267	16
14.) ΣN/ΣP	Weathering [28]	−21	−5	−21	1	21	−13	−11	9	9	3	−20	−21	21
15.) ΣC/ΣP	Weathering [34]	23	16	25	53	4	−14	13	17	FP	43	FP	−14	53
16.) C2N/C1P	Weathering [26]	1	2	−6	7	68	−10	0	18	−19	0	15	−19	68
17.) ΣN/ΣC	Weathering [35]	−56	−25	−63	−15	19	6	−28	−9	FP	−68	FP	−68	19
18.) ΣP/ΣC	Weathering [36]	−29	−20	−34	−114	−3	23	−15	−20	FP	−74	FP	−114	23
19.) ΣD/ΣC	Weathering [34]	15	5	−44	63	69	44	47	14	FP	−53	FP	−53	69
20.) ΣF/ΣC	Weathering [34]	12	29	17	41	83	59	33	17	FP	11	FP	11	83

(*Continued*)

Table 1. Continued.

Ratio	Application	Coal tar								Crude oil				
		CTIL	SOIL	CTNC	SDNY1	SDNY2	SOWI1	SOWI2	SOWI3	ME	OR	AR	Min	Max
21.) C/ΣC	Weathering [37]	−83	−46	−82	−36	−13	−7	−34	−33	FP	ND	FP	−83	−7
22.) C1C/ΣC	Weathering [33]	−11	−25	−35	−30	0	−10	−29	1	FP	15	FP	−35	15
23.) C2C/ΣC	Weathering [33]	17	75	−35	67	2	−4	FP	−25	FP	−89	FP	−89	75
24.) C3C/ΣC	Weathering [33]	ND	ND	FP	FP	−3	FP	FP	FP	ND	ND	ND	−3	−3
25.) Σ(N + F + P + D)/ Σ(P + D)	Weathering [34]	−11	2	−4	17	17	9	−21	9	−1	10	1	−21	17
Min		−556	−2719	−82	−82	−1969	−539	−155	−75	−63	−89	−45		
Max		54	83	64	64	76	59	47	26	95	43	37		

Notes: 1. Bias calculated as follows: $\frac{\text{Ratio}_{\text{SIM}} - \text{Ratio}_{\text{MFPPH}}}{\text{Ratio}_{\text{MFPPH}}} \times 100$.

2. CT = Coal tar, SO = Coal tar-contaminated soil, SD = Coal tar-contaminated sediment.
3. IL = Illinois, NC = North Carolina, NY = New York, WI = Wisconsin.
4. ME = Merey, AR = Arabian, OR = Orinoco.
5. C = Chrysene, D = Dibenzothiophene, N = Naphthalene, P = Phenanthrene, Pyr = Pyrene.
6. ND = Not detected by either method.
7. FP = Signal acquired by SIM, but ion traces fail to comaximise or meet MFPPH relative abundance criteria.
8. Pyrogenic Index = the relative ratio of the sum of the other EPA priority three- to six-ring PAH divided by the sum of the alkylated naphthalene, phenanthrene, dibenzothiophene, fluorene, and chrysene homologues.
9. Σ = Sum of homologues, i.e. Σ(C) = all C_1, C_2, C_3, and C_4 Chrysene homologues.

Table 2. SIM/2-ion vs. MFPPH diagnostic ratio percent bias.

		Coal tar								Crude oil				
Ratio	Application	CTIL	SOIL	CTNC	SDNY1	SDNY2	SOWI1	SOWI2	SOWI3	ME	OR	AR	Min	Max
1.) ΣC/ΣD	Biodegradation	14	−13	34	−64	−168	−16	−90	5	FP	34	FP	−168	34
2.) [ΣN + Σ(C0–C3) DBT + (1/2*Σ(C0–C1) P) + Σ(C2–C4)P]/ΣPAH	Biodegradation	−15	0	36	22	−2	−13	−7	22	−9	−21	−16	−21	36
3.) Pyrogenic Index	Pyrogenic vs. Petrogenic Source	−38	−10	−28	−48	−35	−28	−24	−24	−63	−56	−44	−63	−10
4.) C2D/C2P//C3D/C3P	Source Allocation	75	72	16	−879	−2288	−14	−25	−74	15	8	37	−2288	75
5.) ΣP/ΣD	Source Allocation	−12	−17	14	−92	−185	−3	−118	−20	−36	−14	9	−185	14
6.) P/ΣP	Source Allocation	−41	−11	−35	−16	−7	−17	−17	−5	−36	−27	−44	−44	−5
7.) C1C/C	Source Allocation	40	14	26	5	12	2	4	26	FP	FP	FP	2	40
8.) C2C/C	Source Allocation	54	0	61	76	14	0	FP	6	FP	FP	FP	0	76
9.) C3C/C	Source Allocation	ND	ND	FP	FP	9	FP	FP	FP	ND	ND	ND	9	9
10.) C1D/C1Pyr	Source Allocation	15	0	0	−5	1	−8	−8	−3	46	16	23	−8	46
11.) Σ(C2–C4)N/ΣPAH	Source Allocation and Weathering	0	9	7	19	45	−12	−3	8	−7	−19	−14	−19	45
12.) C1P/ΣP	Source Allocation and Weathering	−30	−5	−31	−11	−6	−3	−8	−1	−14	−15	−45	−45	−1
13.) C1D/ΣD	Source Allocation and Weathering	−23	−23	−14	−123	−201	−16	−155	−26	16	−12	1	−201	16
14.) ΣN/ΣP	Weathering	−21	−7	−29	−4	24	−10	−14	14	9	0	−19	−29	24
15.) ΣC/ΣP	Weathering	23	4	23	14	4	−12	13	21	FP	43	FP	−12	43
16.) C2N/C1P	Weathering	1	2	−3	−5	68	−10	0	18	−19	0	16	−19	68
17.) ΣN/ΣC	Weathering	−56	−11	−69	−21	19	1	−31	−9	FP	−75	FP	−75	19
18.) ΣP/ΣC	Weathering	−29	−4	−31	−17	−6	11	−15	−27	FP	−74	FP	−74	11
19.) ΣD/ΣC	Weathering	−16	11	−51	39	63	13	47	−5	FP	−53	FP	−53	63

(*Continued*)

Table 2. Continued.

Ratio	Application	Coal tar								Crude oil				
		CTIL	SOIL	CTNC	SDNY1	SDNY2	SOWI1	SOWI2	SOWI3	ME	OR	AR	Min	Max
20.) ΣF/ΣC	Weathering	9	28	7	41	83	54	30	17	FP	11	FP	7	83
21.) C/ΣC	Weathering	−83	−16	−77	−36	−13	−5	−34	−33	FP	ND	FP	−83	−5
22.) C1C/ΣC	Weathering	−11	1	−32	−30	0	−3	−29	1	FP	15	FP	−32	15
23.) C2C/ΣC	Weathering	17	−16	31	67	2	−5	FP	−25	FP	−89	FP	−89	67
24.) C3C/ΣC	Weathering	ND	ND	FP	FP	−3	FP	FP	FP	ND	ND	ND	−3	−3
25.) Σ(N + F + P + D)/ Σ(P + D)	Weathering	−6	−1	−8	8	19	10	−24	53	−1	10	−1	−24	53
Min		−83	−23	−77	−879	−2288	−28	−155	−74	−63	−89	−45		
Max		75	72	61	76	83	54	47	53	46	43	37		

Notes: 1. Bias calculated as follows: $\frac{\text{Ratio}_{SIM} - \text{Ratio}_{MFPPH}}{\text{Ratio}_{MFPPH}} \times 100$.

2. CT = Coal tar, SO = Coal tar-contaminated soil, SD = Coal tar-contaminated sediment.
3. IL = Illinois, NC = North Carolina, NY = New York, WI = Wisconsin.
4. ME = Merey, AR = Arabian, OR = Orinoco.
5. C = Chrysene, D = Dibenzothiophene, N = Naphthalene, P = Phenanthrene, Pyr = Pyrene.
6. ND = Not detected by either method.
7. FP = Signal acquired by SIM, but ion traces fail to comaximise or meet MFPPH relative abundance criteria.
8. Pyrogenic Index = the relative ratio of the sum of the other EPA priority three- to six-ring PAH divided by the sum of the alkylated naphthalene, phenanthrene, dibenzothiophene, fluorene, and chrysene homologues.
9. Σ = Sum of homologues, i.e. Σ(C) = all C_1-, C_2, C_3, and C_4 Chrysene homologues.

thousands of percent. These biases are dependent on whether the homologue is in the numerator or denominator of the diagnostic. Examples of incorrect peak assignments for the alkylated 3-ring PASH used in $C_1D/\Sigma D$ (ratio #13) in sample SOWI2 are provided in Figures S1–S3 in the supplemental material available online at http://informahealthcare.com/doi/suppl/[10.1080/03067319.2013.840886]. The figures display ion chromatograms *m/z* 198 (C_1), 212 (C_2), and 226 (C_3) for correctly assigned peaks (green star) and those that failed to meet the criteria for compound identity (red X). The non-homologue peaks contribute to the overestimation of the C_2 and C_3 3-ring PASH, and, in turn, increase the concentrations in the denominator of the ratio.

Nearly 50% of the diagnostic ratios were affected by overestimated homologue concentrations or false positives. In general, higher-order (C_3 and C_4) alkylated PAH and PASH homologues were more affected than the lower order (C_1 and C_2) homologues. These results are consistent with Figure 1. Diagnostic ratio differences were more prevalent in the weathered (sediment) samples than non-weathered (oil) samples, but many false positives were seen in the crude oil results. Nonetheless, no systematic error was observed in the diagnostic ratio differences; thus, we suspect that measurement bias is matrix-dependent. As errors are indiscriminate, no simple correction factor is able to relate SIM to MFPPH results.

Table 2 lists the diagnostic ratio biases obtained from the SIM/2-ion and MFPPH measured concentrations. Although in some cases the addition of a confirming ion to establish compound identity dramatically improved results, see, for example, the alkylated phenanthrene to dibenzothiophene ratio ($\Sigma P/\Sigma D$, ratio #5), which dropped from –479% to –92% for sediment SDNY1, nearly three-quarters of the differences in diagnostic ratios are similar, if not identical, to those of SIM/1-ion analyses. Notably, false positives did not decrease when only one confirming ion was added to identify target compounds. As expected, the more complex the matrix, the higher the likelihood that too few ions will lead to concentration overestimation and false positives.

Based on the analysis of 11 coal tar and crude oil samples, not a single diagnostic ratio was unaffected; see minima and maxima in the tables. These altered diagnostic ratios can have significant repercussions on site investigations, as seen in the following examples. As C_1-phenanthrene weathers more slowly than C_2-naphthalene, the C_2-naphthalene/C_1-phenanthrene ratio (ratio #16) is indicative of the extent of weathering between locations caused by site-specific environmental factors. Selection of this ratio as an indicator of weathering was made, in part, because the molecular ions for these homologues were believed to be less affected by matrix interferences [26]. However, differences in the homologue concentration by SIM compared to MFPPH produced increases in the ratio as high as 68%. The ratio of the naphthalene homologue concentrations divided by the phenanthrene homologue concentrations ($\Sigma N/\Sigma P$, ratio #14) is also used to determine the extent of weathering, as the former can be influenced by the local environment faster than the latter. Six SIM/1-ion samples and five SIM/2-ion samples produced larger increases in ΣN compared to ΣP concentrations than the corresponding MFPPH results. This finding would lead to positively biased ratios and incorrect conclusions that the samples are less weathered than they actually are. For the remaining samples, the naphthalene to phenanthrene ratio decreased, suggesting the samples are more weathered than they actually are. The former could lead to unnecessary cleanup, the latter to a declaration the site is clean when it is not.

Investigators use double ratio plots to determine weathering and to differentiate source materials [10,14,27,33]. An example of a double ratio plot used to assess source allocation is (C2D/C2P)/(C3D/C3P). As the degradation rates of these homologues are similar, this diagnostic ratio should be relatively constant over time. Of all diagnostics examined in this study, double ratio plots were the most affected by SIM overestimation. Figure 4 shows the double ratio plot for the samples. For three samples (Orinoco, Merey, SOWI2), the SIM and MFPPH data are located closely to one another. For example, the Orinoco plot points are located within the dashed

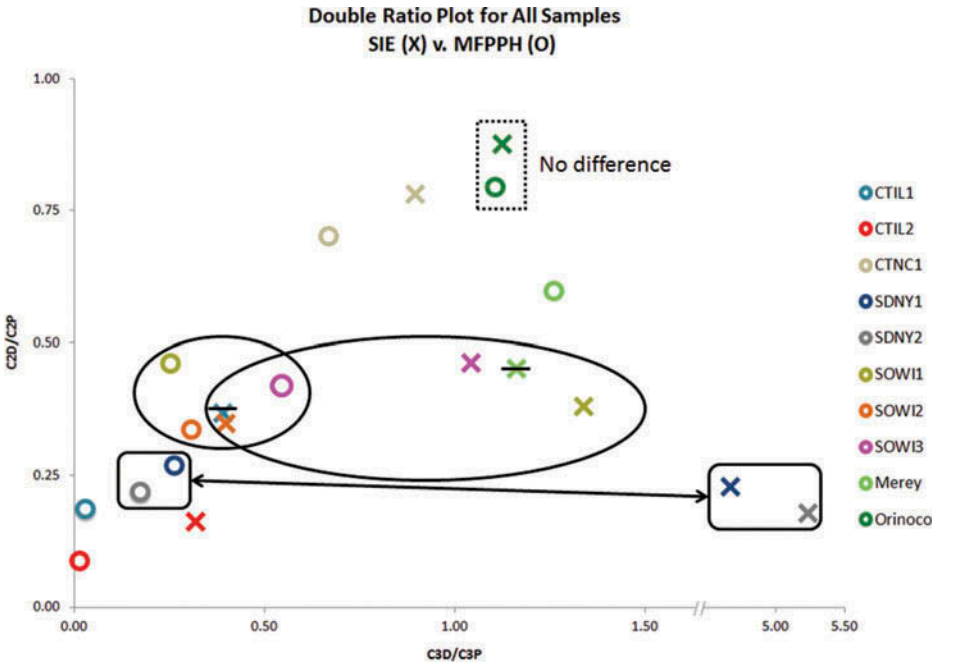

Figure 4. C2D/C2P//C3D/C3P double ratio plot of samples analysed by SIM and MFPPH.

rectangle in the figure. In contrast, the other seven samples have much different SIM and MFPPH plot coordinates, see rounded rectangle for illustration. These two coal tar contaminated sediments, although collected from the same site, have widely different *x*-axis coordinates when calculated by SIM and MFPPH. The result is consistent with the finding that the two data analysis methods produce greatly different C_3 homologue concentrations. The MFPPH double ratio plot points for the coal tar contaminated soils from the same site in Wisconsin cluster together as they should, see oval in figure. In contrast, the SIM data are spread throughout the plot.

Relative distribution histograms are also used to 'fingerprint' oil spills and elucidate source types [14]. Investigators draw conclusions based on the distribution of concentrations amongst parent and alkylated homologues. For example, when homologue concentrations are $C_1>C_2>C_3>C_4$, the source is pyrogenic. In contrast, a bell-shaped distribution is indicative of a petrogenic source. Figure 5 depicts the PAH distribution for a coal tar contaminated sediment, SDNY2. The top histogram, data calculated by MFPPH, exhibits a downward slope, indicating homologue distributions characteristic of a pyrogenic tar. The bottom histogram, produced by SIM, exhibits a change in the 'fingerprint' owing to overestimated homologue concentrations. An example of this overestimation is seen in Figure S4, which shows the SIM ion traces for the C_1-C_4 3-ring PASH for the same sample. As seen in the figure, the C_3 and C_4 homologues (as depicted by their 1-ion traces) are more abundant than the C_1 and C_2 homologues, and as such, more concentrated. However, many of these SIM peaks are attributable to matrix interferences, and as such, are eliminated by MFPPH analysis (see peaks marked by red Xs), leading to lower concentrations and corresponding profile features that indicate a coal tar sample. The SIM alkylated fluorene profile appears bell-shaped and the 2-ring and 3-ring PASH C_3 and C_4 homologue concentrations are higher than those found by MFPPH, so interpretation could suggest the presence of a mixed plume.

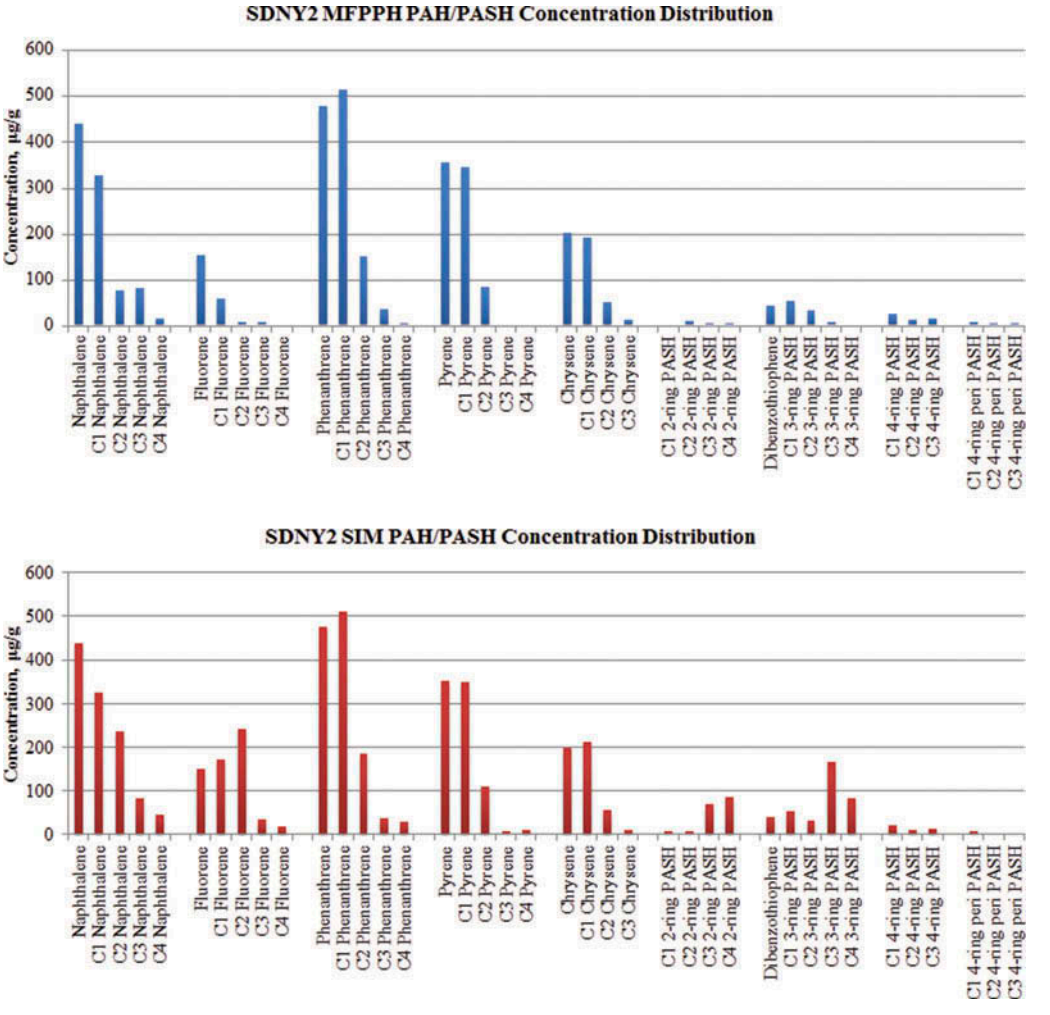

Figure 5. SIM and MFPPH relative distribution histograms of a coal tar contaminated sediment, SDNY2.

The results of this study support our contention that analyses of alkylated PAH and PASH homologues should require the same identification criteria, i.e., multiple ions and their relative abundances, as is widely-accepted for PAH analysis. Employing too few ions eliminates the two-dimensional information content inherent in GC/MS data. Full-scan or SIM analysis using the MFPPH ions and abundances (SIM/MFPPH) eliminates the need to recognise chromatographic patterns of the many isomers comprising each homologue, which can dramatically change from one sample to the next owing to matrix effects. The preference of SIM versus full-scan MS is centred on the question of sensitivity. However, increasing sensitivity at the expense of accuracy is inconsistent with the science of chemical measurements. The aim of this paper is not to critique SIM analysis, only the use of too-few ions to provide unambiguous identification of target analytes. A forthcoming paper will demonstrate that SIM using MFPPH ions is a logical next step toward providing selective, sensitive, accurate, and precise data.

Acknowledgements

The authors appreciate the assistance of Gerstel (GmbH and USA), Agilent Technologies, and Shimadzu for their contribution of instrumentation used in this research. Also appreciated are the utilities that provided samples for this project.

References

[1] *Procedures for the Derivation of ESBs for the Protection of Benthic Organisms: PAH Mixtures, EPA/600/R-02/01* (United States Environmental Protection Agency Office of Research and Development, Washington, DC, 2003).
[2] *Methods for the Derivation of Site-Specific Equilibrium Partitioning Sediment Guidelines (ESGs) for the Protection of Benthic Organisms: Non-Ionic Organics*, *EPA/822/R/02/042* (US Environmental Protection Agency Office of Science and Technology, Washington, DC, 2004).
[3] M. Tobiszewski and J. Namiesnik, Environ. Pollut. **162**, 110 (2012).
[4] S.B. Hawthorne, D.J. Miller and J.P. Kreitinger, Environ. Toxicol. Chem. **25**, 287 (2006).
[5] P.S. Daling, L.G. Faksness, A.B. Hansen and S.A. Stout, Environ. Forensics **3**, 263 (2002).
[6] National Research Council of the National Academies, *Oil in the Sea III: Inputs, Fates, and Effects*, (The National Academies Press, Washington, DC, 2003).
[7] U.H. Yim, M. Kim, S.Y. Ha, S. Kim and W.J. Shim, Environ. Sci. Technol. **46**, 6431 (2012).
[8] M.C. Kennicutt II, Oil Chem. Pollut. **4**, 89 (1988).
[9] W. Youngblood and M. Blumer, Geochim. Cosmochim. Acta **39**, 1303 (1975).
[10] Z. Wang, M. Fingas and D.S. Page, J. Chromatogr. A **843**, 369 (1999).
[11] G.S. Douglas, A.E. Bence, R.C. Prince, S.J. McMillen and E.L. Butler, Environ. Sci. Technol. **30**, 2332 (1996).
[12] *Test Methods for Evaluating Solid Waste*, *SW-846* (United States Environmental Protection Agency, Washington, DC, 1986).
[13] J.W. Short, T.L. Jackson, M.L. Larsen and T.L. Wade, in *Proceedings of the Exxon Valdez Oil Spill Symposium,* edited by S.D. Rice, R.B. Spies, D.A. Wolfe, and B.A. Wright (American Fisheries Society, Bethesda, MD, 1996).
[14] G.S. Douglas, S.D. Emsbo-Mattingly, S.A. Stout, A.D. Uhler and K.J. McCarthy, in *Introduction to Environmental Forensics*, edited by B.L. Murphy and R.D. Morrison (Elsevier Academic Press, Burlington, MA, 2007).
[15] *National Coastal Condition Assessment: Laboratory Methods Manual, EPA/841/R-09/002* (United States Environmental Protection Agency, Washington, DC, 2010).
[16] C.D. Zeigler, M.M. Schantz, S. Wise and A. Robbat, Jr., Polycyclic. Aromat. Compd. **32**, 154 (2012).
[17] *Standard Test Method for Determination of Parent and Alkyl Polycyclic Aromatics in Sediment Pore Water Using Solid-Phase Microextraction and Gas Chromatography/Mass Spectrometry in Selected Ion Monitoring Mode*, *D7363–11* (ASTM International, West Conshohocken, PA 2011).
[18] *Sampling and Analytical Methods of the National Status and Trends Program*, *NOAA Technical Memorandum NOS ORCA 130* (National Oceanic and Atmospheric Administration, Silver Spring, MD, 1998).
[19] C.D. Zeigler, N.D. Wilton and A. Robbat, Jr., Anal. Chem. **84**, 2245 (2012).
[20] C.D. Zeigler and A. Robbat, Jr., Environ. Sci. Technol. **46**, 3935 (2012).
[21] C.D. Zeigler, K. MacNamara, Z. Wang and A. Robbat, Jr., J. Chromatogr. A. **1205**, 109 (2008).
[22] T. Schade and J.T. Andersson, J. Chromatogr. A **1117**, 206 (2006).
[23] L.J. Baldwin, M.L. Tedjamulia, J.G. Stuart, R.N. Castle and M.L. Lee, J. Heterocyclic. Chem. **21**, 1775 (1984).
[24] A. Robbat, Jr., A. Kowalsick and J. Howell, J. Chromatogr. A. **1218**, 5531 (2011).
[25] A.H. Hegazi and J.T. Andersson, Energy Fuels. **21**, 3375 (2007).
[26] W.J. Havenga and E.R. Rohwer, Polycyclic Aromat. Compd. **22**, 327 (2002).
[27] R. Fernandez-Varela, J.M. Andrade, S. Muniategui and D. Prada, J. Chromatogr. A. **1217**, 8279 (2010).
[28] T.C. Sauer, J. Michel, M.O. Hayes and D.V. Aurand, Environ. Int. **24**, 43 (1998).
[29] Z. Wang, M. Fingas, S. Blenkinsopp, G. Sergy, M. Landriault, L. Sigouin, J. Foght, K. Semple and D.W.S. Westlake, J. Chromatogr. A. **809**, 89 (1998).
[30] Z. Wang, M. Fingas and L. Sigouin, J. Chromatogr. A. **909**, 155 (2001).

[31] P.D. Boehm, G.S. Douglas, W.A. Burns, P.J. Mankiewicz, D.S. Page and A.E. Bence, Mar. Pollut. Bull. **34**, 599 (1997).
[32] D.S. Page, P.D. Boehm, G.S. Douglas and A.E. Bence, in *Exxon Valdez Oil Spill: Fate and Effects in Alaska Waters*, edited by P.G. Wells, J.N. Butler, and J.S. Hughes (ASTM International, Philadelphia, PA, 1995).
[33] Z. Wang and M. Fingas, J. Chromatogr. A. **774**, 51 (1997).
[34] S.A. Stout and Z. Wang, in *Oil Spill Environmental Forensics: Fingerprinting and Source Identification,* edited by Z. Wang and S.A. Stout (Academic Press, Burlington, MA, 2007).
[35] Z. Wang, M. Fingas and K. Li, J. Chromatogr. Sci. **32**, 367 (1997).
[36] Z. Wang, M. Fingas and G. Sergy, Environ. Sci. Technol. **29**, 2622 (1995).
[37] T.C. Sauer and P.D. Boehm, *MSRC Technical Report Series 95-032: Hydrocarbon Chemistry Analytical Methods for Oil Spill Assessments* (Marine Spill Response Corporation, Washington, DC, 1995).